Chemical Geology 429 (2016) 85–92

Contents lists available at ScienceDirect

Chemical Geology

journal homepage: www.elsevier.com/locate/chemgeo

Sedimentary chromium isotopic compositions across the Cretaceous OAE2 at Demerara Rise Site 1258

Xiangli Wang [a,*], Christopher T. Reinhard [b], Noah J. Planavsky [a], Jeremy D. Owens [c], Timothy W. Lyons [d], Thomas M. Johnson [e]

[a] Department of Geology and Geophysics, Yale University, New Haven, CT, USA
[b] School of Earth and Atmospheric Sciences, Georgia Institute of Technology, Atlanta, GA, USA
[c] Department of Earth, Ocean, and Atmospheric Science, Florida State University, Tallahassee, FL, USA
[d] Department of Earth Sciences, University of California, Riverside, CA, USA
[e] Department of Geology, University of Illinois at Urbana-Champaign, Urbana, IL, USA

ARTICLE INFO

Article history:
Received 5 September 2015
Received in revised form 12 February 2016
Accepted 9 March 2016
Available online 10 March 2016

Keywords:
OAE2
Chromium isotope
Redox proxy
Trace metals

ABSTRACT

In order to advance our understanding of the emerging chromium (Cr) isotope system as a paleoredox proxy, we measured the $^{53}Cr/^{52}Cr$ of black shales deposited before, during, and after Cretaceous Oceanic Anoxic Event 2 (OAE2). We observed a >1‰ coherent negative $^{53}Cr/^{52}Cr$ excursion and significant drawdown in Cr enrichments during OAE2 coincident with a large positive carbon isotope excursion. Our observed negative $^{53}Cr/^{52}Cr$ excursion during OAE2 is most easily linked to an increase in the ratio of euxinic to reducing conditions. Additional work on other OAE sections is needed to determine the spatial significance of this Cr isotope trend.

1. Introduction

Marine redox changes are closely linked to secular and oscillatory climate shifts, marine nutrient disturbances, and life evolution (Sarmiento et al., 1998; Saltzman, 2005; Holland, 2006; Knoll and Sperling, 2014; Lyons et al., 2014; Planavsky et al., 2014). Previous paleoredox reconstructions (e.g., Meyer and Kump, 2008; Lyons et al., 2009; Poulton and Canfield, 2011) have focused primarily on relatively extreme redox states such as euxinic ($[O_2] = [Fe(II)] = 0, [S(-II)] > 0$) or ferruginous bottom waters ($[O_2] = S(-II) = 0, [Fe(II)] > 0$). However, reducing bottom waters that are conducive to nitrate or manganese reduction but are neither ferruginous nor euxinic) (see Canfield and Thamdrup, 2009), such as those within oxygen minimum zones (OMZs), account for much larger proportions of the predominantly oxic modern marine environment. Sediments underlying reducing bottom waters are potentially very important in controlling globally integrated fluxes of a wide range of oceanographic tracers, and may be expected to respond very sensitively to large changes in ocean chemistry and circulation. Yet few geochemical tools are suited to delineating the roles of reducing settings in structuring ocean chemistry and elemental isotope mass balance. Here, we present the first attempt of using the emerging chromium isotope system to track the evolution of reducing bottom waters.

Chromium is a transition metal with two dominant valence states: Cr(VI) and Cr(III). At circum-neutral pH, Cr(VI) is soluble while Cr(III) is sparingly soluble (Rai et al., 1989), although some Cr(III) can be solubilized by organic ligands (Nakayama et al., 1981). During global Cr biogeochemical cycling (Fig. 1), the insoluble Cr(III) in continental rocks is first oxidized to soluble Cr(VI) during oxidative weathering. The oxidation is extremely sluggish, but can be catalyzed by manganese oxides (e.g. Eary and Rai, 1987; Fendorf and Zasoski, 1992). The oxidized mobile Cr(VI), along with a small amount of organic-bound Cr(III), moves into rivers, eventually reaching the ocean as its primary Cr source. Within the ocean, Cr(VI) is primarily removed from seawater through reduction to insoluble Cr(III), with a small amount of Cr removed by other processes, such as adsorption to oxides and clay minerals, and uptake by biomineralization (e.g., Jeandel and Minster, 1987). Natural Cr(VI) reductants include ferrous iron (e.g. Fendorf and Li, 1996; Sedlak and Chan, 1997), iron sulfide (Patterson et al., 1997), hydrogen sulfide (Kim et al., 2001), organic substances (Wittbrodt and Palmer, 1996), and microbial metabolism (e.g. Wielinga et al., 2001). Although the standard redox potential of the Cr(III)–Cr(VI) couple indicates that reduction of Cr(VI) requires iron reducing conditions, some microorganisms can reduce Cr(VI) under denitrifying conditions (Murray et al., 1983).

* Corresponding author at: 210 Whitney Ave, New Haven, CT 06511, USA.
E-mail address: xiangli.wang@yale.edu (X. Wang).

http://dx.doi.org/10.1016/j.chemgeo.2016.03.006
0009-2541/

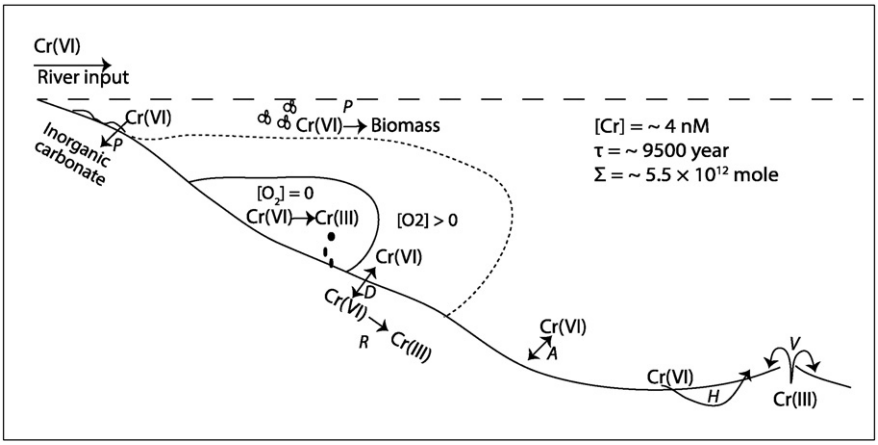

Fig. 1. A cartoon showing a simplified Cr cycle in the modern ocean. The area surrounded by the dotted border represents the Oxygen Minimum Zones (OMZs), with the oxygen being the lowest in the center surrounded by the solid curve. The letters A, D, H, P, R, and V refer to adsorption, diffusion, hydrothermal alteration of oceanic basalt, coprecipitation, reduction, and submarine volcanism. References: [Cr] from Jeandel and Minster, 1987; Cr residence time (τ) and ocean reservoir size (Σ) from Reinhard et al., 2013.

The magnitude of chromium isotope fractionation depends on the redox state of the overlying water column. When the water column is anoxic and contains ferrous iron or hydrogen sulfide, Cr(VI) can be quickly and quantitatively removed, leaving no apparent isotope fractionation (Frei et al., 2009; Reinhard et al., 2014). In contrast, if the water column is reducing, water-column Cr(VI) reduction can be partial (Murray et al., 1983), and thus leads to appreciable Cr isotope fractionation. Furthermore, in areas of high productivity (e.g. OMZs), the sediments could be reducing even though the bottom water could be partially oxic. In these areas, Cr(VI) can diffuse into the sediments to be reduced. The remaining, isotopically fractionated Cr(VI) then diffuses upward to mix with the overlying water column. During partial reduction, lighter isotopes (e.g. ^{52}Cr relative to ^{53}Cr) preferentially enter into the products, pushing the remaining solution to higher ^{53}Cr/^{52}Cr (e.g. Ellis et al., 2002; Schauble et al., 2004; Basu et al., 2014; Reinhard et al., 2014; Wang et al., 2015). The size of the isotope fractionation depends primarily on the length of diffusional transport relative to the kinetics of reduction (Bender, 1990; Clark and Johnson, 2008; Reinhard et al., 2014). Based on these premises, Cr isotopes have provided new insights into the oxygenation of the Early Earth (Frei et al., 2009; Crowe et al., 2013; Planavsky et al., 2014), and have served as a monitor for remediating Cr(VI) contamination in groundwater (e.g. Ellis et al., 2002; Wanner et al., 2011; Izbicki et al., 2012).

The Cr isotope system as a paleoredox proxy has mostly been applied to marine redox evolution when the ocean–atmosphere system was first transitioning from a complete anoxic to a partially oxic state (Frei et al., 2009; Crowe et al., 2013; Planavsky et al., 2014). To advance our understanding of using the Cr isotope system to track marine redox fluctuation during the Phanerozoic, a period when marine redox has varied from being oxic to dysoxic to fully anoxic on a variety of spatio-temporal scales, we have explored one of the most well-constrained global perturbations to marine redox and Earth's carbon cycle in the rock record—the Cenomanian–Turonian Oceanic Anoxic Event (OAE2).

2. Oceanic Anoxic Events

Oceanic Anoxic Events (OAEs) were first defined by Schlanger and Jenkyns (1976) based on recognition of widespread distribution of coeval organic-rich shales during the Mesozoic Era. Black shales deposited during OAEs are thought to record geologically rapid climate events and concomitant biotic extinctions (Jenkyns, 2010). Enhanced primary productivity and a warm climate in the Mesozoic lead to expansion of euxinic deep seawaters (Arthur and Sageman, 1994; Jenkyns, 2010). These anoxic conditions, in turn, favor organic preservation, leading to large organic and inorganic positive carbon isotope excursions during OAEs (Turgeon and Creaser, 2008 and references therein). However, the extent of reducing deep water across OAEs has been less well understood. Specifically, it is yet to be determined whether expansion of anoxia occurred at the cost, or with concurrent expansion of reducing waters.

Among the Mesozoic OAEs, the one spanning the Cenomanian–Turonian Boundary (93.55 Ma, Sageman et al., 2006)—referred to as OAE2—is one of the most widespread and well-studied (e.g. Arthur and Sageman, 1994; Jenkyns, 2010). The duration of the event, however, is still debated, ranging from 240 kyr to 885 kyr (Kuhnt et al., 1997; Sageman et al., 1997; 2006; Prokoph et al., 2001). Although multi-proxy analyses have pointed to widespread anoxia during OAE2 (Damsté and Köster, 1998; Kuypers et al., 2002; Pancost et al., 2004), recent geochemical data and modeling suggest that the expanded euxinia was still limited to a relatively small proportion of the ocean (Owens et al., 2013).

3. Samples

During Ocean Drilling Program Leg 207, cores were drilled at Site 1258 on the Demerara Rise (latitude = 9°26.000′ N and longitude = 54°43.999′ W, water depth = 3192.2) (Shipboard Scientific Party, 2004) (Fig. 2). The sediments were deposited on a passive-margin as Africa and South America separated during the early Cretaceous (Shipboard Scientific Party, 2004). Three drill cores (1258A–C) from this site recovered sediment successions deposited from the Albian to the middle Eocene, which can be divided into 5 lithostratigraphic units. Samples in this study were taken from unit IV (393.73–449.56 mcd, or meters composite depth, MacLeod et al., 2008). Unit IV is comprised of finely laminated calcareous clays with organic matter (5 to 30%, see Hetzel et al., 2006; 2009), and clayey chalk and limestone with organic matter. Fossils include well-preserved shells, occasional phosphorus nodules, and rare concretionary limestone nodules. The OAE2 interval (422–426 mcd) is clearly delineated by a ~6‰ positive δ^{13}C excursion preserved locally in sedimentary organic matter (Erbacher et al., 2005). Pyrite morphology in the OAE2 black shale interval is largely framboidal (Hetzel et al., 2009), indicating an absence of post-depositional sulfide alteration.

4. Methods

Powdered samples were ashed for ~12 h at 450 °C and then completely digested with a combined HF–HNO_3–HCl procedure (see Reinhard et al., 2014). All acids were trace-metal grade. Chromium, molybdenum, titanium, and other element concentrations were determined via ICP-MS analysis on an Agilent 7500-ce in collision cell

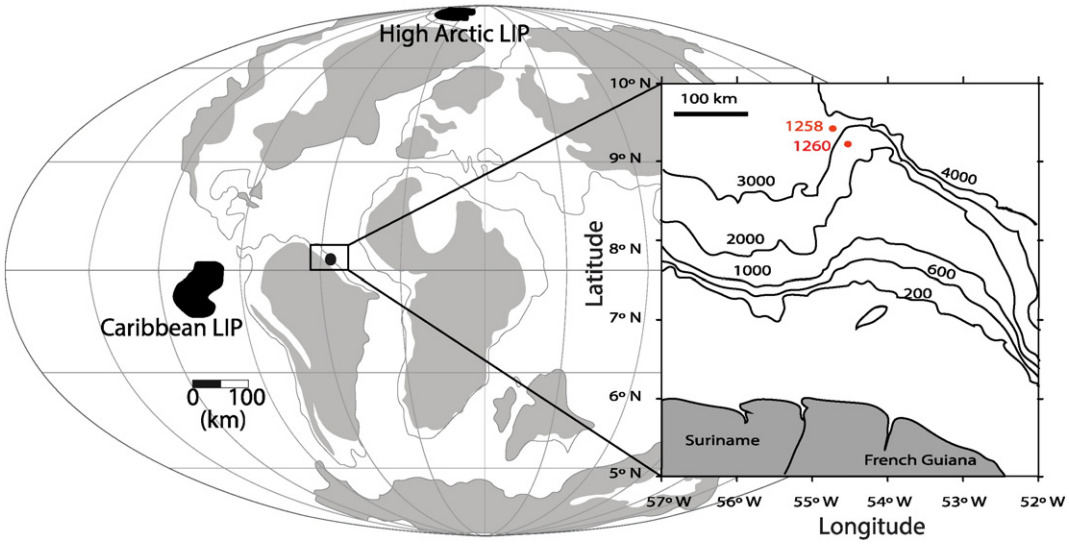

Fig. 2. Location of ODP sites 1258 and 1260 plotted on a paleogeographic map reconstructed for ~90 Ma, modified from Du Vivier et al. (2014). Our Cr isotope data are from Site 1258; previous Os isotope data (Turgeon and Creaser, 2008; Du Vivier et al., 2014) are from Site 1260. The rectangle shows the details of the Demerara Rise where the cores were taken. Also shown are the contemporaneous large igneous provinces (LIP).

mode. The measured Cr concentration was used to calculate the amount of ^{54}Cr–^{50}Cr double spike (composition provided in Wang et al., 2016) to add to samples before ion exchange column chemistry. The ^{54}Cr–^{50}Cr double spike technique corrects artificial fractionation during sample preparation and analysis (Ellis et al., 2002; Schoenberg et al., 2008).

Chromium was purified from sample matrix following methods in Schoenberg et al. (2008). Briefly, spiked sample aliquots were slowly evaporated to dryness, and then redissolved in 0.025 N HCl and 0.02 M $(NH_4)_2S_2O_8$. The sample solutions were heated in sealed Teflon beakers at 130 °C on hot plates for 2 h to oxidize all Cr to chromate. Cooled samples were centrifuged and the supernatants were directly loaded onto pre-cleaned Bio-Rad PolyPrep columns charged with 2 mL AG1-X8 resin (100–200 mesh). Matrix elements were eluted by 0.2 N HCl and 2 N HCl. Chromate was then reduced and rinsed off the resin by 2 N HNO_3 doped with 0.5% (v/v) H_2O_2.

The purified Cr was dissolved in 0.3 N HNO_3 with 250 ppb [Cr] for isotope measurement on a Nu Plasma MC-ICP-MS. The solution was introduced to the plasma via a desolvation nebulizer (Nu Plasma DSN 100). The instrument was set at pseudo-high resolution mode to avoid polyatomic interferences at masses 52 ($^{40}Ar^{12}C$), 53 ($^{40}Ar^{13}C$), and 54 ($^{40}Ar^{14}N$) (Weyer and Schwieters, 2003). Trace amount of ^{54}Fe, ^{50}Ti, and ^{50}V was corrected for based on ^{56}Fe, ^{49}Ti, and ^{51}V signals and natural abundances ($^{54}Fe/^{56}Fe = 15.6979$; $^{50}Ti/^{49}Ti = 0.9586$; $^{50}V/^{51}V = 0.0024$).

Measurements consisted 5 blocks of 50 cycles, each cycle lasting 4.19 s. True $^{53}Cr/^{52}Cr$ ratios were extracted from raw ratios using an iterative method described in Johnson et al. (1999). Extracted $^{53}Cr/^{52}Cr$ ratios are converted to $\delta^{53}Cr$ by normalizing to standard NIST SRM 979.

Data quality was ensured by measuring blanks, processed NIST SRM 3112a, and processed USGS BHVO-2. Unprocessed NIST SRM 979 was also run every three samples to monitor instrument drift. The blank level ranged from 10–20 ng, which was negligible compared to the 1–2 μg sample Cr. Processed NIST SRM 3112a and USGS BHVO-2 returned -0.01 ± 0.07‰ (2 s.d., n = 6) and -0.13 ± 0.09‰ (2 s.d., n = 12), respective, consistent with previous studies (Schoenberg et al., 2008). The 2 s.d. of USGS BHVO-2 (0.09‰) is used as the external uncertainty for the $\delta^{53}Cr$ values reported in this study.

Measured $\delta^{53}Cr$ can be corrected for detrital component to obtain the authigenic $\delta^{53}Cr$, according to:

$$\delta^{53}Cr_{\text{auth}} = \left(\delta^{53}Cr_{\text{bulk}} - \delta^{53}Cr_{det}(1 - f_{\text{auth}})\right)/f_{\text{auth}} \quad (1)$$

where $\delta^{53}Cr_{auth}$, $\delta^{53}Cr_{bulk}$, *and* $\delta^{53}Cr_{det}$ refer to the Cr isotopic compositions for the authigenic, bulk, and detrital components, respectively. Further, f_{auth} refers to the fraction of authigenic Cr, defined as:

$$f_{\text{auth}} = \left([\text{Cr}]_{\text{bulk}} - [\text{Ti}]_{\text{bulk}}(\text{Cr/Ti})_{det}\right)/[\text{Cr}]_{\text{bulk}} \quad (2)$$

where $[Cr]_{auth}$, $[Cr]_{bulk}$, $[Ti]_{bulk}$, and $(Cr/Ti)_{det}$ correspond to the authigenic Cr concentration, bulk Cr concentration, bulk Ti concentration, and the Cr/Ti ratio of detrital sediments. The $(Cr/Ti)_{det}$ can be estimated by the value of the upper continental crust (0.016–0.024) (Condie, 1993; McLennan, 2001; Rudnick and Gao, 2003), although its value may slightly vary geographically (more below).

5. Results

We found striking systematic negative excursions in $\delta^{53}Cr$ and trace element enrichments during the OAE2 interval (Table 1 and Fig. 3). The redox sensitive elements Cr and Mo are reported as Cr/Ti and Mo/Ti ratios to avoid potential complication due to varying sedimentation rate and carbonate dilution effects. The trajectories of $\delta^{53}Cr$, Cr/Ti, and Mo/Ti correlate well with previously reported $\delta^{13}C$ excursion obtained in the same cores (Erbacher et al., 2005).

The $\delta^{53}Cr_{bulk}$ values stayed relatively constant before OAE2 with an average bulk value of ~1.2‰, dropped to as low as ~0.2‰ with the onset of OAE2, and then subsequently rebounded slowly to the pre-OAE2 value (Fig. 3B). We observe a small transient decrease in both $\delta^{53}Cr$ and Cr/Ti just prior to the onset of OAE2. This transient shift, however, is very small relative to the major excursion. In addition, a slight time offset between $\delta^{13}C$–$\delta^{53}Cr$–[Mo] and [Cr] trends is also observed.

The $\delta^{53}Cr_{bulk}$ is positively correlated with Cr/Ti (Fig. 4A) when Cr/Ti is lower than ~0.12, but $\delta^{53}Cr_{bulk}$ reaches a plateau when Cr/Ti is higher than ~0.12. The $\delta^{53}Cr$ appears to be negatively correlated with total organic content, especially at high TOC concentrations (Fig. 4B). The Cr and Mo enrichments are muted at low TOC levels, reaches a maximum at ~10% TOC, and return to low values at high TOC content (Fig. 4C and D).

6. Discussion

The observed negative $\delta^{53}Cr$ excursion has three potential end-member explanations: (1) seawater $\delta^{53}Cr$ decreased due to non-redox processes (hydrothermal, riverine input, seawater heterogeneity); (2) seawater $\delta^{53}Cr$ remained constant throughout OAE2, and the

Table 1
Geochemical results for black shale samples from ODP Leg 207 Site 1258. Sample label follows the convention of "leg-site&hole core-section interval". Age model is constructed using a sedimentation rate of 0.9 cm/kyr (Sageman et al., 2006; MacLeod et al., 2008). The authigenic fraction (f_{auth}) is estimated using crustal Cr/Ti values of 0.03 (Methods section).

Sample label	Depth	Age	TOC	[Cr]	[Ti]	[Mo]	$\delta^{53}Cr_{bulk}$	$\delta^{53}Cr_{auth}$	f_{auth}
	(mcd)	Ma	%	μg g^{-1}	μg g^{-1}	μg g^{-1}	‰	‰	–
207-1258A 42-4 18–20 cm	418.89	93.30	13.52	96.7	694.9	106.6	1.20	1.56	0.75
207-1258A 42-4 117.5–119 cm	419.89	93.41	13.42	56.9	822.6		0.72	1.35	0.49
207-1258B 45R-3 1–2 cm	420.19	93.44	11.24	77.6	1289.9	135.6	0.70	1.49	0.42
207-1258A 42-5 51–53 cm	420.68	93.49	16.45	44.3	588.0		0.82	1.43	0.54
207-1258A 42-5 119–121 cm	421.36	93.57	8.39	28.3	417.4		0.62	1.19	0.48
207-1258B 45-4 30–31 cm	421.89	93.63	10.40	71.5	753.6	83.6	0.99	1.49	0.63
207-1258B 45R-4 40–41 cm	421.99	93.64	7.12	72.9	620.5	57.4	0.89	1.23	0.70
207-1258A 42-6 82–83 cm	422.31	93.68	19.86	39.9	654.0	52.3	0.37	0.83	0.43
207-1258A 42-6 113–114 cm	422.62	93.71	18.84	67.1	955.4		0.66	1.23	0.50
207-1258B 45R-4 106–107 cm	422.65	93.71	14.63	89.5	1121.9	60.0	0.58	0.99	0.56
207-1258A 42-7 10–11 cm	422.99	93.75	20.60	77.8	1338.0		0.65	1.45	0.40
207-1258B 45R-4 148–149 cm	423.07	93.76	13.55	70.7	1108.0	29.7	0.27	0.60	0.45
207-1258A 42-7 100–101 cm	423.89	93.85	17.27	62.6	1624.0		0.32	1.79	0.09
207-1258C 17R-1 5–6 cm	424.84	93.96	20.81	76.1	1217.3	28.5	0.24	0.55	0.44
207-1258C 17R-1 80–81 cm	425.59	94.04	14.39	99.3	2728.7	29.3	0.25	1.87	0.04
207-1258C 17R-2 12–13 cm	426.30	94.12	7.11	51.9	511.1	91.5	1.11	1.61	0.66
207-1258C 17R-2 25–26 cm	426.43	94.13	11.04	187.4	748.3	82.4	1.23	1.41	0.86
207-1258C 17R-2 70–71 cm	426.88	94.18	4.47	46.5	412.2	67.2	0.86	1.21	0.69
207-1258C 17R-2 105–106 cm	427.23	94.22	5.93	109.7	777.9	59.0	1.05	1.36	0.75
207-1258C 17R-3 4–5 cm	427.42	94.24	1.80	30.0	291.8	25.9	1.06	1.54	0.66
207-1258C 17R-3 25–26 cm	427.63	94.27	11.73	248.0	1046.4	105.2	1.26	1.45	0.85
207-1258C 17R-3 45–46 cm	427.83	94.29	10.92	190.2	752.2	101.6	1.27	1.45	0.86
207-1258C 17R-CC 2–3 cm	427.98	94.31	11.85	197.4	798.7	95.1	1.22	1.41	0.86
207-1258C 17R-CC 15–16 cm	428.11	94.32	13.96	166.3	684.4	113.0	1.26	1.45	0.86
207-1258A 43-2 39–41 cm	428.15	94.32	12.85	155.3	786.3		1.20	1.43	0.82
207-1258A 43-3 2–3 cm	429.04	94.42	12.04	233.4	1289.0		1.14	1.39	0.81
207-1258A 43-3 68.5–70 cm	429.71	94.50	7.26	113.6	465.8	73.8	1.08	1.25	0.86
207-1258A 43-4 10–12 cm	430.17	94.55	9.70	116.7	676.2		1.14	1.40	0.80
207-1258A 43-4 39–40.5 cm	430.46	94.58	10.45	61.8	624.6	145.9	1.03	1.52	0.65
207-1258A 43-4 69–70 cm	430.76	94.61	11.71	195.2	698.3	53.3	1.13	1.28	0.87

observed drop in sedimentary $\delta^{53}Cr$ was caused by increased detrital contribution; (3) seawater $\delta^{53}Cr$ decreased due to ocean redox shifts.

6.1. Hydrothermal input of isotopically light Cr

Mantle Cr sources are expected to have high Cr content and slightly negative $\delta^{53}Cr$ values (-0.1 ± 0.1‰, Schoenberg et al., 2008; Farkaš et al., 2013). Therefore, one possible hypothesis for the negative Cr isotope excursion during OAE2 is an increased flux of isotopically light Cr from submarine hydrothermal activities (Holmden et al., 2014). However, if this were true, Cr concentration in sediments should increase significantly during active hydrothermal events, but the opposite is observed.

Another evidence against the hydrothermal hypothesis is the decoupling between $\delta^{53}Cr$ and $^{187}Os/^{188}Os$ excursions. Sharp drop in $^{187}Os/^{188}Os$ during OAE2 has been attributed to large igneous provinces (e.g., Turgeon and Creaser, 2008; Du Vivier et al., 2014). However, the $^{187}Os/^{188}Os$ excursion predates the major $\delta^{53}Cr$ excursion by ~23 kyr (Turgeon and Creaser, 2008) (Fig. 3). Furthermore, the minor $\delta^{53}Cr$

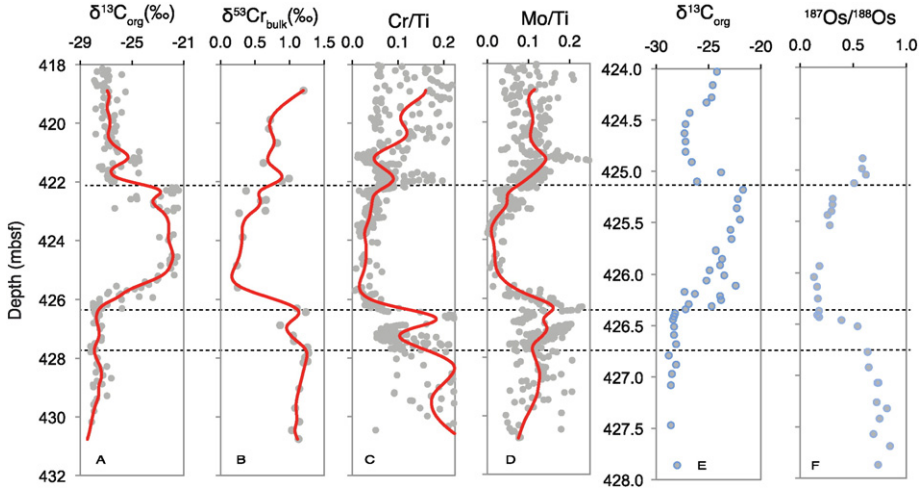

Fig. 3. Geochemical results across the Cenomanian–Turonian boundary at Site 1258 (A–D) and Site 1260 (E–F). Note that A–D and E–F have different vertical scales. $\delta^{53}Cr$ from Site 1258 and $^{187}Os/^{188}Os$ from Site 1260 are correlated using $\delta^{13}C$ excursions from the two sites. The upper two dashed lines delineate the OAE2 interval. The third dashed line delineates the first minor excursion in $\delta^{53}Cr$. Notice the time offset between two $\delta^{53}Cr$ excursions and the $^{187}Os/^{188}Os$ excursion. Data sources: carbon isotopes for Site 1258 from Erbacher et al., 2005;. Carbon and osmium isotopes for Site 1260 from Turgeon and Creaser (2008) and Du Vivier et al. (2014).

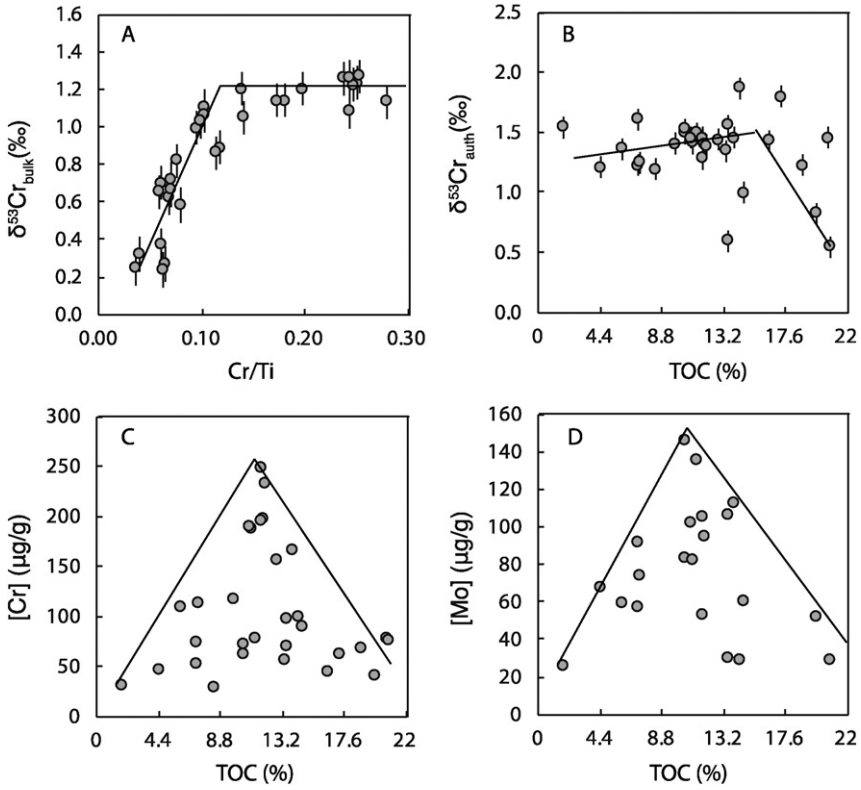

Fig. 4. Cross plots between $\delta^{53}Cr_{bulk}$ and Cr/Ti (A), between $\delta^{53}Cr_{auth}$ and TOC (B), between [Cr] and TOC (C), and between [Mo] and TOC. The plateau in A represents the average authigenic Cr value mixed with detrital contamination. The zenith in B represents the best estimate for the authigenic Cr. The triangle shapes in the plots of Cr and Mo vs. TOC indicate that redox-sensitive trace metal enrichments at Demerara Site 1258 were controlled not solely by TOC. The low Cr–Mo enrichments at high TOC content were likely due to drawdown of seawater metal reservoir due to expanded ocean euxinia.

excursion before the major one is not matched with a $^{187}Os/^{188}Os$ counterpart.

6.2. Changes in riverine flux and isotope composition

The primary pathway of Cr removal from seawater is via reduction of Cr(VI) to insoluble Cr(III) (Jeandel and Minster, 1987). Partial reduction preferentially removes lighter Cr isotopes leading to more positive seawater $\delta^{53}Cr$ values. As a result, our working hypothesis is that seawater $\delta^{53}Cr$ values will be heavier than the globally integrated riverine input to the oceans. Thus, another potential mechanism for shifting seawater toward light $\delta^{53}Cr$ values is by increasing the overall input flux. However, at a constant seawater redox state, seawater $\delta^{53}Cr$ should recover to the initial state shortly after (a few Cr residence time, ~20–50 kyr) the increased input flux, which is in contrast to the >200 kyr OAE2 during which seawater $\delta^{53}Cr$ was persistently shifted to much lower values. Further, this mechanism should also increase the seawater Cr inventory, which is inconsistent with the observed drop in Cr enrichments (Fig. 3E).

Another possibility is a shift toward lighter $\delta^{53}Cr$ values in the globally integrated riverine input. Existing experimental data suggest that oxidation of Cr(III) induces −2.5‰ to +1.1‰ isotope fractionation, depending on the phases of manganese oxides (Bain and Bullen, 2005; Zink et al., 2010; Joshi et al., 2011). However, river waters measured so far all have positive $\delta^{53}Cr$ values, ranging from +0.2‰ to +3.9‰ (Farkaš et al., 2013; Frei et al., 2014), which is clearly fractionated from the igneous rocks (−0.1 ± 0.1‰, Schoenberg et al., 2008; Farkaš et al., 2013). Therefore, one plausible mechanism for shifting river water $\delta^{53}Cr$ to lighter values is by shifting weathering toward more congruent dissolution that induces smaller isotope fractionation. Indeed, recent lithium isotope data suggest a global shift toward more congruent weathering at the onset of OAE2 (von Strandmann et al., 2013), and this effect would have pushed river $\delta^{53}Cr$ values toward the bulk silicate Earth value. However, we note that "congruency" may not necessarily mean the same for Cr and Li, given that the former is redox dependent while the latter is not. For Cr, the isotopic composition of the weathering flux is driven toward positive $\delta^{53}Cr$ values by some combination of oxidative, incongruent weathering processes (Frei and Polat, 2012; Crowe et al., 2013) and partial reduction of Cr(VI) during subsurface transport in watersheds (e.g., Ellis et al., 2002; Berna et al., 2010; Izbicki et al., 2012). Although we cannot conclusively rule out changes in either of these terrestrial processes during OAE2, there is no reason to believe they would have undergone the drastic changes required to lower river $\delta^{53}Cr$ by nearly 1‰.

6.3. Impacts of marine Cr isotope heterogeneity

Recent seawater data reported by Scheiderich et al. (2015) suggest that modern surface seawater is heterogeneous in $\delta^{53}Cr$. However, the isotopic heterogeneity seems to be confined to the surface water, as deep water masses with different sources in open Atlantic and Pacific oceans have similar $\delta^{53}Cr$ values (~0.5 ± 0.1‰, Bonnand et al., 2011; Scheiderich et al., 2015). Further, the Beaufort Sea investigated by Scheiderich et al. (2015) is a quasi-isolated basin with limited communication with open seawater; therefore, the heavier deep-water $\delta^{53}Cr$ values in this region (~1.1 ± 0.1‰) may not represent the deep water of the open ocean. However, given that Cr concentration across OAE2 was significantly lower and thus Cr residence time should have been shorter than in the modern world, heterogeneous seawater $\delta^{53}Cr$ during OAE2 may be a significant issue.

Therefore, one explanation for the observed $\delta^{53}Cr$ excursion may be shifting water masses carrying different $\delta^{53}Cr$ signals. Indeed, systematic changes in Nd isotope values throughout OAE2 at the same site explored here does suggest changing water masses throughout the

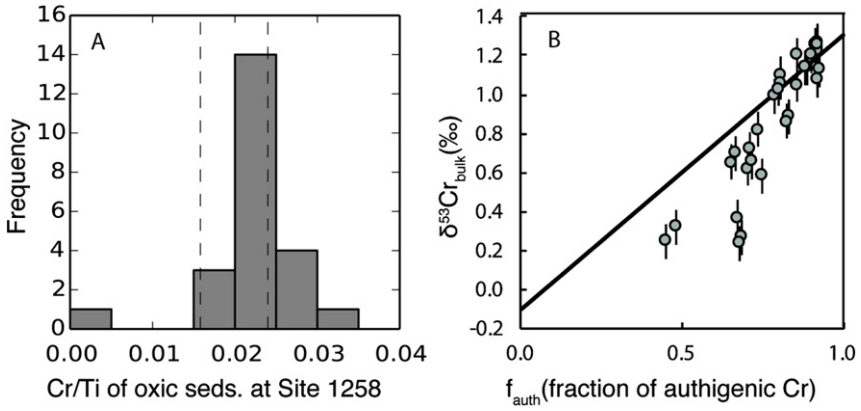

Fig. 5. A histogram of Cr/Ti in oxic sediments at Site 1258 (0–330 mcd) (A), and δ^{53}Cr plotted against the fraction of authigenic Cr (B). In A, the vertical dashed lines represent the estimated range for the average upper continental crust (Condie, 1993; McLennan, 2001; Rudnick and Gao, 2003). The Cr/Ti in the oxic section is used to correct for detrital component from the bulk δ^{53}Cr. The Cr/Ti from the oxic section of Site 1258 appears to be slightly higher than the estimated range for the upper continental crust, which could be due to slight authigenic enrichment by adsorption. The solid line in B represents a two-endmember mixing between detrital component (δ^{53}Cr value of ~−0.1‰ (Schoenberg et al., 2008; Farkaš et al., 2013) and authigenic component (δ^{53}Cr value of ~1.5‰). The mismatch between the mixing model and observed data suggests that enhanced dilution by detrital Cr cannot explain the negative δ^{53}Cr excursion during OAE2.

event (MacLeod et al., 2008). However, shifting water masses should have resulted in synchronous shifts in seawater Cr concentration and δ^{53}Cr value, which contradicts with the time offset observed between excursions for δ^{53}Cr and Cr enrichment (Fig. 3).

6.4. Evaluating the effect of detrital dilution on the negative δ^{53}Cr excursion

As mentioned above, the detrital input is isotopically lighter than the seawater. Therefore, the negative δ^{53}Cr excursion during the OAE2 interval could be due to increased detrital dilution. This hypothesis can be tested by a simple two-endmember mixing model (δ_{mix}) between detritally sourced Cr (δ_{det}, -0.1 ± 0.1‰, Schoenberg et al., 2008; Farkaš et al., 2013) and authigenic Cr (δ_{auth}):

$$\delta_{mix} = f_{auth} \cdot \delta_{auth} + (1 - f_{auth}) \cdot \delta_{det}. \quad (3)$$

The δ_{auth} value can be approximated by the plateau value in Fig. 4B (δ_{auth} = ~1.5‰). The δ_{det} is based on a suite of pelagic siliciclastic sediments (Schoenberg et al., 2008; Reinhard et al., 2014). The f_{auth} value is given by Eq (2) using an $(Cr/Ti)_{det}$ value of 0.022, based on the oxic sediments at Site 1258 (Fig. 5A, data from Hetzel et al., 2006). This value is consistent with the average upper continental crust (Condie, 1993; McLennan, 2001; Rudnick and Gao, 2003). There are no major or trace element characteristics (e.g., Sr/Ti and Ti/Al, Hetzel et al., 2006) that would suggest a major shift in weathering intensity or provenance between sediments in the OAE2 interval and the overlying oxic sediments. Therefore, the Cr/Ti ratio from the oxic section can be applied to the investigated section.

Fig. 5B shows that a simple two-endmember mixing between detrital and authigenic Cr cannot fit all of the observed δ^{53}Cr. This suggests that redox condition, rather than detrital dilution, influenced the Cr isotope fractionation during sequestering into the sediments at Site 1258.

6.5. Implications for seawater redox

Extensive geochemical evidences have pointed to persistent bottom water euxinia throughout the investigated section (Hetzel et al., 2009). Euxinia is marked by strong sedimentary Cr and Mo enrichments throughout the section, except within the OAE2 interval, when Cr and Mo dropped. Paleontological evidence indicates that occasional short-lived oxic events occurred within OAE2, but these events are unlikely to have had a major effect on bulk geochemical signals (Hetzel et al., 2009). The observed drop in redox-sensitive trace metal enrichments during peak OAE2 can been attributed to depletion of seawater metal reservoir due to expansion of the spatial extent of seawater euxinia (Hetzel et al., 2009). Therefore, the Cr isotope trend in the examined interval at Site 1258 is not likely to be controlled by local redox state (there was euxinia before, during, and after the peak OAE). Although the observed drop in δ^{53}Cr could be tied in part to decreased Cr enrichments—and thus a greater detrital Cr contribution, detrital dilution is not the sole explanation for the δ^{53}Cr excursion (see above).

We propose that the observed negative δ^{53}Cr excursion is linked to a decrease in seawater δ^{53}Cr values. A drop in seawater δ^{53}Cr would require burying less isotopically light Cr (keeping river input the same; see above). This requires an increase in the amount of Cr removed through near quantitative reduction, which is expected in euxinic conditions (e.g. Reinhard et al., 2014; see above). In this light, the observed sedimentary δ^{53}Cr drop can be linked to an increase in euxinic water at the expense of reducing waters (where Cr burial will be accompanied by an isotope fractionation) during the onset of OAE2. This interpretation could be confirmed by trying to reproduce our results from other OAE2 sections.

Recent results from Scheiderich et al. (2015) reported heterogeneous seawater δ^{53}Cr, meaning the Cr isotopes may only serve as a regional redox proxy. The residence time of Cr in the modern ocean (with 4 nM total Cr, see Reinhard et al., 2013) is ~9 kyr, which is longer than the ocean mixing time of ~1 kyr (Broecker and Peng, 1982), but still much shorter than other well-known global redox proxies (Mo and U). Seawater Cr heterogeneity would be particularly true under extremely low Cr concentrations like those during OAE2. Therefore, assuming the δ^{53}Cr excursion is linked to an increase in euxinic waters at the expense of reducing waters, additional modeling and geochemical work on other OAE2 sections is needed to determine the spatial significance (local vs. regional vs. global) of the observed Cr isotope exchange.

Acknowledgment

This research was supported by Agouron Postdoctoral Fellowship, NASA Exobiology & Evolutional Biology Program, and the NASA Astrobiology Institute and the NSF Earth-Life Transitions Program. The authors thank editor Michael E. Böttcher, reviewer Thomas Algeo, and two anonymous reviewers for constructive comments that greatly improved the quality of the manuscript.

References

Arthur, M., Sageman, B., 1994. Marine black shales: depositional mechanisms and environments of ancient deposits. Annu. Rev. Earth Planet. Sci. 22, 499–551.

Bain, D.J., Bullen, T.D., 2005. Chromium isotope fractionation during oxidation of Cr (III) by manganese oxides. Geochim. Cosmochim. Acta 69, S212.

Basu, A., Johnson, T.M., Sanford, R.A., 2014. Cr isotope fractionation factors for Cr (VI) reduction by a metabolically diverse group of bacteria. Geochim. Cosmochim. Acta 142, 349–361.

Bender, M.L., 1990. The $\delta^{18}O$ of dissolved O_2 in seawater: A unique tracer of circulation and respiration in the deep sea. J. Geophys. Res. Oceans 95, 22243–22252.

Berna, E.C., Johnson, T.M., Makdisi, R.S., Basu, A., 2010. Cr stable isotopes as indicators of Cr (VI) reduction in groundwater: a detailed time-series study of a point-source plume. Environ. Sci. Technol. 44, 1043–1048.

Bonnand, P., Parkinson, I.J., James, R.H., Karjalainen, A.-M., Fehr, M.A., 2011. Accurate and precise determination of stable Cr isotope compositions in carbonates by double spike MC-ICP-MS. J. Anal. At. Spectrom. 26, 528–535.

Broecker, W., Peng, T., 1982. Tracers in the Sea. Lamont-Doherty Geol. Obs, Palisades, NY, USA.

Canfield, D., Thamdrup, B., 2009. Towards a consistent classification scheme for geochemical environments, or, why we wish the term 'suboxic'would go away. Geobiology 7, 385–392.

Clark, S.K., Johnson, T.M., 2008. Effective isotopic fractionation factors for solute removal by reactive sediments: A laboratory microcosm and slurry study. Environ. Sci. Technol. 42, 7850–7855.

Condie, K.C., 1993. Chemical composition and evolution of the upper continental crust: contrasting results from surface samples and shales. Chem. Geol. 104, 1–37.

Crowe, S.A., Døssing, L.N., Beukes, N.J., Bau, M., Kruger, S.J., Frei, R., Canfield, D.E., 2013. Atmospheric oxygenation three billion years ago. Nature 501, 535–538.

Damsté, J.S.S., Köster, J., 1998. A euxinic southern North Atlantic Ocean during the Cenomanian/Turonian oceanic anoxic event. Earth Planet. Sci. Lett. 158, 165–173.

Du Vivier, A.D., Selby, D., Sageman, B.B., Jarvis, I., Gröcke, D.R., Voigt, S., 2014. Marine $^{187}Os/^{188}Os$ isotope stratigraphy reveals the interaction of volcanism and ocean circulation during Oceanic Anoxic Event 2. Earth Planet. Sci. Lett. 389, 23–33.

Eary, L.E., Rai, D., 1987. Kinetics of chromium (III) oxidation to chromium (VI) by reaction with manganese dioxide. Environ. Sci. Technol. 21, 1187–1193.

Ellis, A.S., Johnson, T.M., Bullen, T.D., 2002. Chromium isotopes and the fate of hexavalent chromium in the environment. Science 295, 2060.

Erbacher, J., Friedrich, O., Wilson, P.A., Birch, H., Mutterlose, J., 2005. Stable organic carbon isotope stratigraphy across Oceanic Anoxic Event 2 of Demerara Rise, western tropical Atlantic. Geochem. Geophys. Geosyst. 6, Q06010.

Farkaš, J., Chrastny, V., Novak, M., Cadkova, E., Pasava, J., Chakrabarti, R., Jacobsen, S.B., Ackerman, L., Bullen, T.D., 2013. Chromium isotope variations ($\delta^{53/52}Cr$) in mantle-derived sources and their weathering products: Implications for environmental studies and the evolution of $\delta^{53/52}Cr$ in the Earth's mantle over geologic time. Geochim. Cosmochim. Acta 123, 74–92.

Fendorf, S.E., Li, G., 1996. Kinetics of chromate reduction by ferrous iron. Environ. Sci. Technol. 30, 1614–1617.

Fendorf, S.E., Zasoski, R.J., 1992. Chromium (III) Oxidation by δ-MnO_2. Environ. Sci. Technol. 26, 79–85.

Frei, R., Polat, A., 2012. Chromium isotope fractionation during oxidative weathering-implications from the study of a Paleoproterozoic (ca. 1.9 Ga) paleosol, Schreiber Beach, Ontario, Canada. Precambrian Res. 224, 434–453.

Frei, R., Gaucher, C., Poulton, S.W., Canfield, D.E., 2009. Fluctuations in Precambrian atmospheric oxygenation recorded by chromium isotopes. Nature 461, 250–253.

Frei, R., Poiré, D., Frei, K.M., 2014. Weathering on land and transport of chromium to the ocean in a subtropical region (Misiones, NW Argentina): a chromium stable isotope perspective. Chem. Geol. 381, 110–124.

Hetzel, A., Brumsack, H.-J., Schnetger, B., Böttcher, M.E., 2006. Inorganic geochemical characterization of lithologic units recovered during ODP Leg 207 (Demerara Rise). Proc. ODP Sci. Results 1–37.

Hetzel, A., Böttcher, M.E., Wortmann, U.G., Brumsack, H.-J., 2009. Paleo-redox conditions during OAE 2 reflected in Demerara Rise sediment geochemistry (ODP Leg 207). Palaeogeogr. Palaeoclimatol. Palaeoecol. 273, 302–328.

Holland, H.D., 2006. The oxygenation of the atmosphere and oceans. Philos. Trans. R. Soc. Lond. Ser. B Biol. Sci. 361, 903–915.

Holmden, C., Jacobson, A.D., Sageman, B.B., Hurtgen, M., 2014. Response of the Cr isotope proxy to Oceanic Anoxic Event 2. Goldschmidt Conference, Sacramento, CA, USA.

Izbicki, J.A., Bullen, T.D., Martin, P., Schroth, B., 2012. Delta Chromium-53/52 isotopic composition of native and contaminated groundwater, Mojave Desert, USA. Appl. Geochem. 27, 841–853.

Jeandel, C., Minster, J., 1987. Chromium behavior in the ocean: global versus regional processes. Glob. Biogeochem. Cycles 1, 131–154.

Jenkyns, H.C., 2010. Geochemistry of oceanic anoxic events. Geochem. Geophys. Geosyst. 11, Q03004.

Johnson, T.M., Herbel, M.J., Bullen, T.D., Zawislanski, P.T., 1999. Selenium isotope ratios as indicators of selenium sources and oxyanion reduction. Geochim. Cosmochim. Acta 63, 2775–2783.

Joshi, S., Wang, D., Ellis, A.S., Johnson, T.M., Bullen, T.D., 2011. Stable Isotope Fractionation During Cr(III) Oxidation by Manganese Oxides. AGU Fall Meeting, San Francisco, CA, U.S.A.

Kim, C., Zhou, Q., Deng, B., Thornton, E.C., Xu, H., 2001. Chromium(VI) reduction by hydrogen sulfide in aqueous media: stoichiometry and kinetics. Environ. Sci. Technol. 35, 2219–2225.

Knoll, A.H., Sperling, E.A., 2014. Oxygen and animals in Earth history. Proc. Natl. Acad. Sci. U. S. A. 111, 3907–3908.

Kuhnt, W., Nederbragt, A., Leine, L., 1997. Cyclicity of Cenomanian–Turonian organic-carbon-rich sediments in the Tarfaya Atlantic coastal basin (Morocco). Cretac. Res. 18, 587–601.

Kuypers, M.M., Pancost, R.D., Nijenhuis, I.A., Sinninghe Damsté, J.S., 2002. Enhanced productivity led to increased organic carbon burial in the euxinic North Atlantic basin during the late Cenomanian oceanic anoxic event. Paleoceanography 17 (pp. 3-1-3-13).

Lyons, T.W., Anbar, A.D., Severmann, S., Scott, C., Gill, B.C., 2009. Tracking euxinia in the ancient ocean: a multiproxy perspective and Proterozoic case study. Annu. Rev. Earth Planet. Sci. 37, 507–534.

Lyons, T.W., Reinhard, C.T., Planavsky, N.J., 2014. The rise of oxygen in Earth's early ocean and atmosphere. Nature 506, 307–315.

MacLeod, K.G., Martin, E.E., Blair, S.W., 2008. Nd isotopic excursion across Cretaceous ocean anoxic event 2 (Cenomanian–Turonian) in the tropical North Atlantic. Geology 36, 811–814.

McLennan, S.M., 2001. Relationships between the trace element composition of sedimentary rocks and upper continental crust. Geochem. Geophys. Geosyst. 2 (pp. 2000GC000109).

Meyer, K.M., Kump, L.R., 2008. Oceanic euxinia in Earth history: causes and consequences. Annu. Rev. Earth Planet. Sci. 36, 251–288.

Murray, J.W., Spell, B., Paul, B., 1983. The contrasting geochemistry of manganese and chromium in the eastern tropical Pacific Ocean. Trace Metals in Sea Water. Springer, pp. 643–669 (vol.).

Nakayama, E., Kuwamoto, T., Tsurubo, S., Tokoro, H., Fujinaga, T., 1981. Chemical speciation of chromium in sea water: Part 1. Effect of Naturally Occurring Organic Materials on the Complex Formation of Chromium (III). Anal. Chim. Acta 130, 289–294.

Owens, J.D., Gill, B.C., Jenkyns, H.C., Bates, S.M., Severmann, S., Kuypers, M.M., Woodfine, R.G., Lyons, T.W., 2013. Sulfur isotopes track the global extent and dynamics of euxinia during Cretaceous Oceanic Anoxic Event 2. Proc. Natl. Acad. Sci. U. S. A. 110, 18407–18412.

Pancost, R.D., Crawford, N., Magness, S., Turner, A., Jenkyns, H.C., Maxwell, J.R., 2004. Further evidence for the development of photic-zone euxinic conditions during Mesozoic oceanic anoxic events. J. Geol. Soc. Lond. 161, 353–364.

Patterson, R.R., Fendorf, S., Fendorf, M., 1997. Reduction of hexavalent chromium by amorphous iron sulfide. Environ. Sci. Technol. 31, 2039–2044.

Planavsky, N.J., Reinhard, C.T., Wang, X., Thomson, D., McGoldrick, P., Rainbird, R.H., Johnson, T., Fischer, W.W., Lyons, T.W., 2014. Low Mid-Proterozoic atmospheric oxygen levels and the delayed rise of animals. Science 346, 635–638.

Poulton, S.W., Canfield, D.E., 2011. Ferruginous conditions: a dominant feature of the ocean through Earth's history. Elements 7, 107–112.

Prokoph, A., Villeneuve, M., Agterberg, F.P., Rachold, V., 2001. Geochronology and calibration of global Milankovitch cyclicity at the Cenomanian–Turonian boundary. Geology 29, 523–526.

Rai, D., Eary, L., Zachara, J., 1989. Environmental chemistry of chromium. Sci. Total Environ. 86, 15–23.

Reinhard, C.T., Planavsky, N.J., Robbins, L.J., Partin, C.A., Gill, B.C., Lalonde, S.V., Bekker, A., Konhauser, K.O., Lyons, T.W., 2013. Proterozoic ocean redox and biogeochemical stasis. Proc. Natl. Acad. Sci. U. S. A. 110, 5357–5362.

Reinhard, C.T., Planavsky, N.J., Wang, X., Fischer, W.W., Johnson, T.M., Lyons, T.W., 2014. The isotopic composition of authigenic chromium in anoxic marine sediments: a case study from the Cariaco Basin. Earth Planet. Sci. Lett. 407, 9–18.

Rudnick, R.L., Gao, S., 2003. In: Turekian, H.D.H.K. (Ed.), Composition of the Continental CrustTreatise on Geochemistry vol. 3. Pergamon, Oxford, pp. 1–64.

Sageman, B., Rich, J., Arthur, M., Birchfield, G., Dean, W., 1997. Evidence for Milankovitch periodicities in Cenomanian–Turonian lithologic and geochemical cycles, Western Interior USA. J. Sediment. Res. 67, 286–302.

Sageman, B.B., Meyers, S.R., Arthur, M.A., 2006. Orbital time scale and new C-isotope record for Cenomanian–Turonian boundary stratotype. Geology 34, 125–128.

Saltzman, M.R., 2005. Phosphorus, nitrogen, and the redox evolution of the Paleozoic oceans. Geology 33, 573–576.

Sarmiento, J.L., Hughes, T.M.C., Stouffer, R.J., Manabe, S., 1998. Simulated response of the ocean carbon cycle to anthropogenic climate warming. Nature 393, 245–249.

Schauble, E., Rossman, G.R., Taylor Jr., H.P., 2004. Theoretical estimates of equilibrium chromium-isotope fractionations. Chem. Geol. 205, 99–114.

Scheiderich, K., Amini, M., Holmden, C., Francois, R., 2015. Global variability of chromium isotopes in seawater demonstrated by Pacific, Atlantic, and Arctic Ocean samples. Earth Planet. Sci. Lett. 423, 87–97.

Schlanger, S., Jenkyns, H., 1976. Cretaceous oceanic anoxic events: causes and consequences. Geol. Mijnb. 55, 179–184.

Schoenberg, R., Zink, S., Staubwasser, M., von Blanckenburg, F., 2008. The stable Cr isotope inventory of solid Earth reservoirs determined by double spike MC-ICP-MS. Chem. Geol. 249, 294–306.

Sedlak, D.L., Chan, P.G., 1997. Reduction of hexavalent chromium by ferrous iron. Geochim. Cosmochim. Acta 61, 2185–2192.

Shipboard Scientific Party, 2004. Leg 207 Summary. Proc. Ocean Drill. Program Initial Rep. 207, 89.

Turgeon, S.C., Creaser, R.A., 2008. Cretaceous oceanic anoxic event 2 triggered by a massive magmatic episode. Nature 454, 323–326.

von Strandmann, P.A.P., Jenkyns, H.C., Woodfine, R.G., 2013. Lithium isotope evidence for enhanced weathering during Oceanic Anoxic Event 2. Nat. Geosci. 6, 668–672.

Wang, X.L., Johnson, T.M., Ellis, A.S., 2015. Equilibrium isotopic fractionation and isotopic exchange kinetics between Cr (III) and Cr (VI). Geochim. Cosmochim. Acta 153, 72–90.

Wang, X.L., Planavsky, N.J., Reinhard, C.T., Zou, H.J., Ague, J.J., Wu, Y.B., Gill, B.C., Schwarzenbach, E.M., Peucker-Ehrenbrink, B., 2016. Chromium isotope fractionation during subduction-related metamorphism, black shal weathering, and hydrothermal alteration. Chem. Geol. 423, 19–33.

Wanner, C., Eggenberger, U., Kurz, D., Zink, S., Mäder, U., 2011. A chromate-contaminated site in southern Switzerland, part 1: Site characterization and the use of Cr isotopes to delineate fate and transport. Appl. Geochem. 27, 644–654.

Weyer, S., Schwieters, J., 2003. High precision Fe isotope measurements with high mass resolution MC-ICP-MS. Int. J. Mass Spectrom. 226, 355–368.

Wielinga, B., Mizuba, M.M., Hansel, C.M., Fendorf, S., 2001. Iron promoted reduction of chromate by dissimilatory iron-reducing bacteria. Environ. Sci. Technol. 35, 522–527.

Wittbrodt, P.R., Palmer, C.D., 1996. Effect of temperature, ionic strength, background electrolytes, and Fe (III) on the reduction of hexavalent chromium by soil humic substances. Environ. Sci. Technol. 30, 2470–2477.

Zink, S., Schoenberg, R., Staubwasser, M., 2010. Isotopic fractionation and reaction kinetics between Cr(III) and Cr(VI) in aqueous media. Geochim. Cosmochim. Acta 74, 5729–5745.